crystals

MDPI

Communication

Crystal Structure of the Protonated Germanide Cluster $[HGe_9]^{3-}$

Corinna Lorenz and Nikolaus Korber *

Institute of Inorganic Chemistry, University of Regensburg, 93055 Regensburg, Germany; Corinna.Lorenz@ur.de
* Correspondence: Nikolaus.Korber@ur.de; Tel.: +49-941-943-4448; Fax: +49-941-943-1812

Received: 28 August 2018; Accepted: 17 September 2018; Published: 21 September 2018

Abstract: A single crystal X-ray diffraction study of the new compound $[Rb([2.2.2]crypt)]_2[Rb([18]crown{-}6)][HGe_9]\cdot 4NH_3$ revealed the presence of the first protonated nine-atom germanide cluster $[HGe_9]^{3-}$. It forms from Rb_4Ge_9 in liquid ammonia, so that $[Ge_9]^{4-}$ can be considered as the base and $[HGe_9]^{3-}$ its formally conjugated acid. The H atom is attached to a germanium vertex atom of the basal square plane, as it is known for $[RGe_9]^{3-}$ (R = C_5H_9, Mes, etc.) or $[HE_9]^{3-}$ (E = Si, Sn). In addition, the proton could be located unambiguously in the Fourier difference map. $[HGe_9]^{3-}$ also represents a nido cluster species with 22 cluster-bonding electrons, which can be considered the most stable structure for nine-atom cluster species for all group 14 elements.

Keywords: Zintl anion; liquid ammonia; crystal structure

1. Introduction

The ability of metals to form negatively charged species was experimentally proven by Joannis in 1891 [1]. Later, Zintl and co-workers determined, by means of electrochemical and potentiometric experiments on solutions of alkali metal alloys of the heavier main group elements in liquid ammonia, that these species must be polyanionic salts [2,3]. However, the shape of the so-called Zintl ions was then still completely unknown. This changed after the introduction of the chelating alkali metal ligand cryptand to these solutions by Corbett [4,5], when the isolation and structural characterization of solvate structures containing Zintl anions was facilitated. At present, for group 14 elements the representative homoatomic cluster anions identified in several solid state and solvate structures are $[E_4]^{4-}$ (E = Si–Pb) [6–9], $[E_5]^{2-}$ (E = Si–Pb) [10–13], $[E_9]^{x-}$ (x = 4; E = Si-Pb; x = 3, E = Si–Sn; x = 2 E = Si,Ge) [5,14–18] and $[E_{10}]^{2-}$ (E = Ge, Pb) [19,20]. For solvation experiments with germanium clusters, A_4Ge_9 (A = K–Cs) [21,22] or $A_{12}Ge_{17}$ (A = Na, K, K/Rb, Rb, Cs) [23,24] phases are used as starting materials, which contain the nine-atom germanide cluster or respectively $[Ge_9]^{4-}$/$[Ge_4]^{4-}$ cage anions in a ratio of 1:2. These compounds are readily soluble in anhydrous liquid ammonia, ethylendiamine or *N*,*N*-dimethylformamide [4,25,26]. Recently, we reported on the synthesis and first structural characterization of the elusive and highly charged $[Ge_4]^{4-}$ anion in $Cs_4Ge_4\cdot 9NH_3$ [7]. However, solution chemistry with the more stable and better characterized $[Ge_9]$ clusters is far better developed. They undergo a variety of reactions with different reagents like transition metal complexes, acyl chlorides or chlorophosphines [5,27–29]. As mentioned above, the $[Ge_9]$ clusters exist with three different overall charges: −4, −3 and −2. Starting with the fourfold negatively charged cluster, the charge of −3 and −2 can either be explained by oxidation (Equation (1)) [30,31] or protonation (Equation (2)) [32].

$$[Ge_9]^{4-} \rightleftarrows [Ge_9]^{3-} + e^- \text{ (solv)} \rightleftarrows [Ge_9]^{2-} + 2e^- \text{ (solv)} \quad (1)$$

$$[Ge_9]^{4-} + 2\,NH_3 \rightleftarrows [HGe_9]^{3-} + NH_3 + {NH_2}^- \rightleftarrows [H_2Ge_9]^{2-} + 2\,{NH_2}^- \quad (2)$$

Sevov et al. assume that $[Ge_9]^{4-}$ clusters are oxidized after dissolution. In solution they are then in an equilibrium with their oxidized species $[Ge_9]^{3-}$ and $[Ge_9]^{2-}$ and solvated electrons (Equation (1)) [31]. An oxidation state of −3 or −2 per $[Ge_9]$ cage can also be observed in dimers $[Ge_9\text{-}Ge_9]^{6-}$ [16,33,34], trimers $[Ge_9{=}Ge_9{=}Ge_9]^{6-}$ [35,36], tetramers $[Ge_9{=}Ge_9{=}Ge_9{=}Ge_9]^{8-}$ [37,38] or in one-dimensionally extended $^1_\infty[\text{-}Ge_9\text{-}]^{2-}$ [39–41] chains, which could be obtained by the oxidative coupling of $[Ge_9]^{4-}$ anions. However, the protonation of $[Ge_9]^{4-}$ clusters is also highly likely (Equation (2)). Here, $[Ge_9]^{4-}$ can be considered as the base and $[HGe_9]^{3-}$ as the formal conjugated acid. For the lighter and the heavier homologous elements of group 14, the formation of $[HSi_9]^{3-}$ and $[HSn_9]^{3-}$ has already been reported in the literature [15,32], as well as $[H_2Si_9]^{2-}$ [42] and a mixed Si/Ge species $[H_2(Si/Ge)_9]^{2-}$ [14]. Thus, it seemed highly likely that pure $[Ge_9]^{4-}$ clusters would also undergo similar protolytic reactions.

2. Results and Discussion

The cluster compound $[Rb([2.2.2]crypt)]_2[Rb([18]crown{-}6)][HGe_9]\cdot 4NH_3$ could be observed after the extraction of Rb_4Ge_9 in liquid ammonia in the presence of two chelating agents [2.2.2]cryptand (4,7,13,16,21,24-hexaoxa-1,10-diazabicyclo[8.8.8]hexacosane) and [18]crown−6 and the organocadmium compound $CdPh_2$ (Appendix A). A single crystal X-ray structure diffraction study clearly revealed the presence of the first protonated nine-atom germanide cluster $[HGe_9]^{3-}$. Next to the anionic cluster, the asymmetric unit also contains three rubidium cations, which are sequestered by [18]crown−6 and [2.2.2]cryptand, and four ammonia molecules of crystallization. $P2_1/n$ could be determined as the space group of the solvate structure. The space group was confirmed using PLATON [43]. In Table 1, the crystal structure and structure refinement details are listed.

Table 1. Crystallographic data of $[Rb([2.2.2]crypt)]_2[Rb([18]crown{-}6)][HGe_9]\cdot 4NH_3$.

Chemical Formula	$[Rb([2.2.2]crypt)]_2[Rb([18]crown{-}6)][HGe_9]\cdot 4NH_3$
CCDC No. *	1858787
Mr [g·mol^{-1}]	1995.14
Crystal system	monoclinic
Space group	$P2_1/n$
a [Å]	13.8629(3)
b [Å]	14.3533(3)
c [Å]	38.8444(6)
α [°]	90
β [°]	95.899(2)
γ [°]	90
V [Å^3]	7688.3(3)
Z	4
F(000) (e)	3960.0
ρ_{calc} [g·cm^{-3}]	1.719
μ [mm^{-1}]	5.415
Absorption correction	numerical [44]
Diffractometer (radiation source)	MoKα (λ = 0.71073)
2θ-range for data collection [°]	6.4–53.464
Reflections collected/independent	130738/16301
Data/restraints/parameters	16301/18/872
Goodness-of-fit on F^2	1.110
Final *R* indices [$I > 2\sigma(I)$]	*R*1 = 0.0476, *w*R2 = 0.0791
R indices (all data)	*R*1 = 0.0762, *w*R2 = 0.0863
R_{int}	0.0923
$\Delta\rho$max, $\Delta\rho$max [*e*·Å^{-3}]	0.76/−0.51

* Crystallographic data have been deposited with the Cambridge Crystallographic Data Centre, CCDC, 12 Union Road, Cambridge CB21EZ, UK. Copies of the data can be obtained free of charge on quoting the depository number CCDC-1858787.

The anionic part of the compound is represented by the $[HGe_9]^{3-}$ cluster (Figure 1), which is the first protonated nine-atom germanide cluster to be reported to date. The Ge-Ge distances within the cage anion are listed in Table 2. The average atomic distance (*d*) has a value of 2.637 Å. This is in good accordance with previously reported germanide clusters [16,18]. The longest Ge-Ge bond lengths can be found in the central square plane (Ge5-Ge6, Ge5-Ge8, Ge6-Ge7, Ge7-Ge8, Table 2).

In contrast, the shortest Ge-Ge atomic distances with values of 2.460(5) Å ((H-Ge1)-Ge2) and 2.529(4) Å ((H-Ge1)-Ge4) are observed in the basal square plane, which involve the germanium atom to which the hydrogen atom is attached. While these two bond lengths are reduced, the opposite two Ge-Ge distances in the basal square plane Ge2-Ge3 = 2.686(6) Å and Ge3-Ge4 = 2.681(6) Å (Figure 1) are elongated. This reaction of the bond lengths of the basal square plane of the cluster is an expected and already documented consequence of any functionalization by exo-bonded ligands [33,45–49]. Figure 2 shows the ligand-free (a,e) [50], protonated (b,f), coupled (c,g) [33] and twofold substituted (d,h) [51] germanide cluster with a view to the basal square plane and each rotated by 90°. The $[Ge_9]^{4-}$ cluster, from which all listed cluster species can be derived, ideally shows C_{4v} symmetry. Its shape can be best described as a one-capped square antiprism (Figure 2a,e). According to Wade´s electron counting rules [52,53], the $[Ge_9]^{4-}$ anion can be considered as a *nido* cluster with $2n + 4 = 22$ cluster-bonding electrons. Protonation, functionalization by one or two ligands or coupling of n $[Ge_9]^{4-}$ anions causes a deviation from that ideal C_{4v} symmetry to approximately C_{2v} or C_s symmetry, as it is for the compound reported here (Figure 2). However, there is no fundamental change of the electronic situation and they remain 22-electron 9-vertex nido cluster species. Overall, the clusters only differ in the level of distortion of the basal square plane [51]. As mentioned above, functionalization by one ligand or protonation causes an elongation and reduction of two Ge-Ge atomic distances in the open face (Figure 2b,c,f,g). Thus, the clusters mostly adopt C_s symmetry. If two ligands are bonded on two facing germanium atoms (Figure 2d), the basal square plane undergoes an even greater compression (Figure 2h). This results in an overall shortening of the Ge-Ge atomic distances and they can be considered almost equal. As a result, the more symmetrical $[R_2\text{-}Ge_9]^{2-}$ clusters mostly adopt approximately C_{2v} symmetry [48,49,54–56].

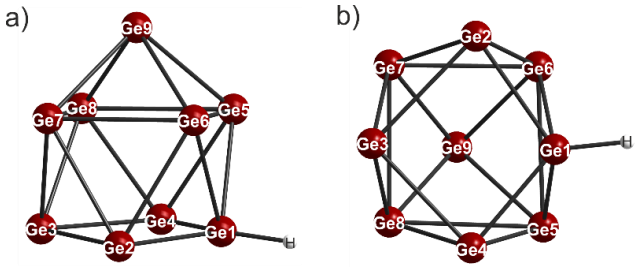

Figure 1. (**a**,**b**) Two different views of the anionic part of the compound $[Rb([2.2.2]crypt)]_2[Rb([18]crown{-}6)][HGe_9]\cdot 4NH_3$.

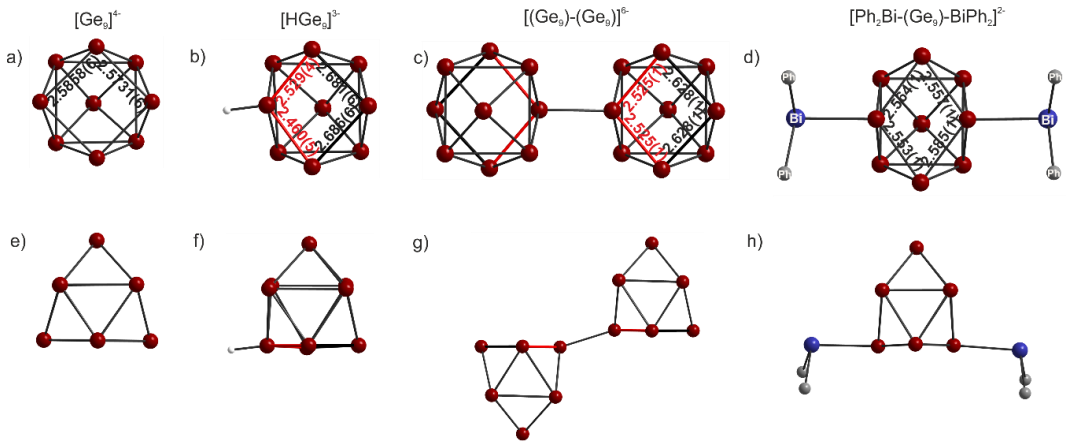

Figure 2. Comparison of different germanide cluster species with view to the basal square plane and rotation by 90°: (**a**,**e**) $[Ge_9]^{4-}$ cluster in [K-(2,2)diaza-[18]-crown-6]$K_3Ge_9\cdot$2en; (**b**,**f**) $[HGe_9]^{3-}$ in $[Rb([2.2.2]crypt)]_2[Rb([18]crown{-}6)][HGe_9]\cdot 4NH_3$; (**c**,**g**) $[(Ge_9\text{-}Ge_9)]^{6-}$ in $Cs_4(K\text{-}crypt)_2[(Ge_9)\text{-}(Ge_9)]\cdot$6en and (**d**,**h**) $[Ph_2Bi\text{-}(Ge_9)\text{-}BiPh_2]^{2-}$ in $(K\text{-}crypt)_2[Ge_9(BiPh_2)_2]\cdot$en.

Table 2. Distances [Å] within the anionic moiety $[HGe_9]^{3-}$.

Atom1-Atom2	Distance (Å)	Atom1-Atom2	Distance (Å)
Ge1-H	1.39(9)	Ge4-Ge8	2.584(7)
Ge1-Ge2	2.460(5)	Ge4-Ge5	2.693(6)
Ge1-Ge4	2.529(4)	Ge5-Ge6	2.852(4)
Ge1-Ge5	2.600(5)	Ge5-Ge8	2.788(7)
Ge1-Ge6	2.558(3)	Ge5-Ge9	2.639(6)
Ge2-Ge3	2.686(6)	Ge6-Ge7	2.758(3)
Ge2-Ge6	2.658(2)	Ge6-Ge9	2.588(4)
Ge2-Ge7	2.553(3)	Ge7-Ge8	2.874(5)
Ge3-Ge4	2.681(6)	Ge7-Ge9	2.579(5)
Ge3-Ge7	2.551(6)	Ge8-Ge9	2.576(6)
Ge3-Ge8	2.539(8)		

The germanide cluster in the described compound shows a slight orientational disorder that could be resolved by a 0.695:0.305 ratio. Due to the high quality of the single crystal X-ray data (Table 1), the proton of the $[HGe_9]^{3-}$ cluster could be located unambiguously on the Fourier difference map. The Ge-H distance of 1.39(9) Å is slightly shorter than the values found in the literature (1.45(3) Å [57]). The proton is also located on a vertex germanium atom of the basal square plane, as it is supposed to be for $[HSn_9]^{3-}$ [32], and found at $[HSi_9]^{3-}$ [14,15].

The threefold negative charge of $[HGe_9]^{3-}$ is compensated by two $[Rb[2.2.2]crypt]^{+}$ and one $[Rb[18]crown–6]^{+}$ complex. Due to the two different chelating agents, the anion and the cations are almost completely separated. Only Rb1 of the $[Rb[18]crown-6]^{+}$ complex shows contact to the anion. It coordinates η_4 like on the basal square plane of the cage, the site where electrophilic substitution is preferred [31]. The Rb-Ge distances range between 3.584(6)–3.740(2) Å. Rb1 is removed by 1.021 Å out of the mean plane of the crown ether molecule with Rb1-O distances of 2.873(3)–3.088(4) Å. Rb2 and Rb3 are sequestered by the [2.2.2]cryptand. The Rb-O distances of 2.846(3)–2.908(3) Å as well as the Rb-N distances of 2.990(3)–3.3.052(4) Å are in good accordance with the values found in the literature [12]. Additionally, there are four ammonia molecules of crystallization. Two of them refine to complete occupancy, the remaining two are 80% and 82% occupied.

Altogether, the $[Rb[2.2.2]crypt]^{+}$ and the $[Rb[18]crown–6]^{+}$ complexes form cavities along the crystallographic *a*- and *b*-axis, where the $[HGe_9]^{3-}$ clusters and the ammonia molecules of crystallization are located (Figure 3).

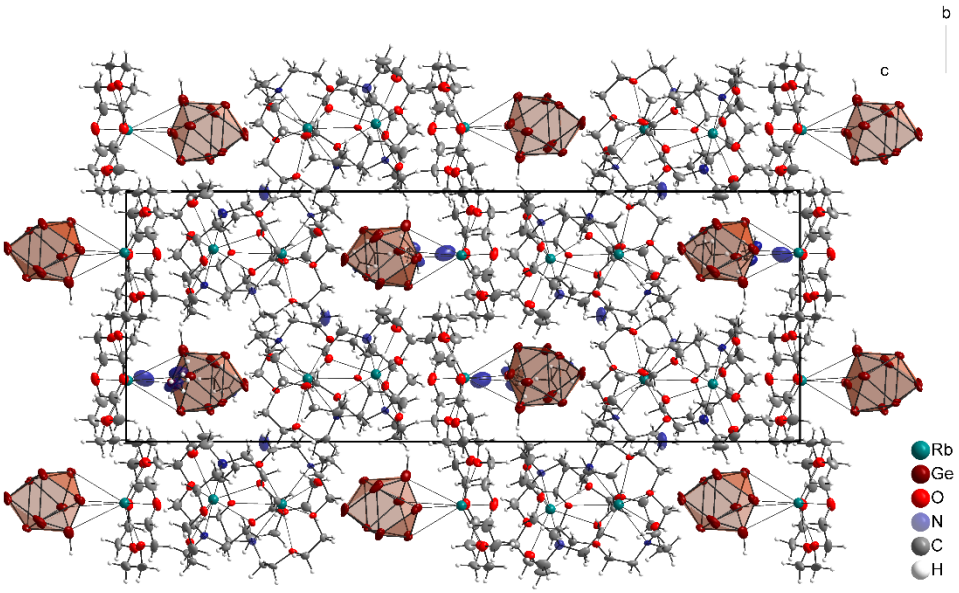

Figure 3. Projection of $[Rb([2.2.2]crypt)]_2[Rb([18]crown-6)][HGe_9]\cdot 4NH_3$ along the crystallographic *a*-axis. Anisotropic displacement ellipsoids at 50% probability level.

3. Conclusions

We were able to synthesize and structurally characterize the first protonated germanide cluster $[HGe_9]^{3-}$ in the compound $[Rb([2.2.2]crypt)]_2[Rb([18]crown{-}6)][HGe_9]\cdot 4NH_3$. The hydrogen atom could be located unambiguously in the Fourier difference map and is bonded to a vertex germanium atom of the basal square plane of the cluster, as has also been reported for the other group 14 species $[HSi_9]^{3-}$ and $[HSn_9]^{3-}$.

Author Contributions: C.L. carried out experimental work (synthesis, crystallization, X-ray structure determination) and prepared the manuscript. N.K. designed and conceived the study.

Funding: This research received no external funding.

Conflicts of Interest: The authors declare no conflict of interest.

Appendix A.

Appendix A.1. Experimental Details

All operations were carried out under an argon atmosphere using standard Schlenk and Glovebox techniques. Liquid ammonia was stored over sodium metal in a dry ice cooled Dewar vessel and was directly condensed on the reaction mixture. Germanium (irregular peaces, 99.999%, 5N, ABCR) was used as received. Rubidium was synthesized according to Hackspill [58] and distilled for purification. [18]crown−6 was sublimated under dynamic vacuum at 353 K. [2.2.2]cryptand (ABCR) was used without further purification. In the reaction mixtures containing the two chelating agents, crystals of the composition $C_{12}H_{24}O_6\cdot 2NH_3$ and $C_{18}H_{36}O_6N_2\cdot 2NH_3$ could also be observed [59].

Appendix A.1.1. Synthesis of $[Rb([2.2.2]crypt)]_2[Rb([18]crown{-}6)][HGe_9]\cdot 4NH_3$

Synthesis of the precursor Rb_4Ge_9: The phase was synthesized via solid-state reaction. Ge (1.313 g, 18.071 mmol) and Rb (0.687 g, 8.035 mmol) were enclosed in tantalum containers and jacketed in an evacuated ampoule of fused silica. The containers were heated to 1223 K at a rate of 25 $K\cdot h^{-1}$. The temperature was maintained for 2 h. The ampoule was cooled down with a rate of 20 $K\cdot h^{-1}$. The precursor was stored in a glovebox under argon.

$[Rb([2.2.2]crypt)]_2[Rb([18]crown{-}6)][HGe_9]\cdot 4NH_3$: 100 mg (0.100 mmol) of the precursor was dissolved in about 15 ml of anhydrous liquid ammonia together with 39.8 mg (0.151 mmol) [18]crown−6, 94.5 mg (0.251 mmol) [2.2.2]cryptand and 26.7 mg (0.100 mmol) $CdPh_2$. The Schlenk tube was stored at 197 K. After several months, very few brownish crystals could be observed. The compound accounts for about 15% of the crystalline yield.

Appendix A.1.2. X-ray Diffraction Studies

The crystals are very temperature and moisture labile. To overcome the difficult handling, a technique developed by Kottke and Stalke, was used [60,61]. Crystals were directly isolated with a micro spatula from the reaction solutions into a recess of a glass slide containing perfluoroether oil, which was cooled by liquid nitrogen steam. Crystals were selected by means of a stereo microscope. An appropriate crystal was attached on a MicroLoop™ and placed on a goniometer head on the diffractometer. In Table 1, details of the single crystal X-Ray structure analysis are listed.

Due to the disorder of the cluster cage and the incomplete occupation of N7 and N8, SIMU restraints were applied. Hydrogen atoms were calculated and refined according to a riding model.

References

1. Joannis, M. Action du sodammonium et du potassammonium sur quelques méteaux. *Hebd. Seances Acad. Sci.* **1891**, *113*, 795–798.

2. Zintl, E.; Goubeau, J.; Dullenkopf, W. Salzartige Verbindungen und Intermetallische Phasen Des Natriums in Flüssigem Ammoniak. *Z. Phys. Chem.* **1931**, *154*, 1–46. [CrossRef]
3. Zintl, E.; Harder, A. Polyplumbide, Polystannide und ihr Übergang in Metallphasen. *Z. Phys. Chem.* **1931**, *154A*, 47–91. [CrossRef]
4. Corbett, J.D. Polyatomic Zintl anions of the post-transition elements. *Chem. Rev.* **1985**, *85*, 383–397. [CrossRef]
5. Scharfe, S.; Kraus, F.; Stegmaier, S.; Schier, A.; Fässler, T.F. Zintl ions, cage compounds, and intermetalloid clusters of group 14 and group 15 elements. *Angew. Chem. Int. Ed.* **2011**, *50*, 3630–3670. [CrossRef] [PubMed]
6. Lorenz, C.; Gärtner, S.; Korber, N. Si_4^{4-} in Solution—First Solvate Crystal Structure of the Ligand-free Tetrasilicide Tetraanion in $Rb_{1.2}K_{2.8}Si_4 \cdot 7NH_3$. *Zeitschrift für Anorganische und Allgemeine Chemie* **2017**, *643*, 141–145. [CrossRef]
7. Lorenz, C.; Gärtner, S.; Korber, N. Ammoniates of Zintl Phases: Similarities and Differences of Binary Phases A_4E_4 and Their Corresponding Solvates. *Crystals* **2018**, *8*, 276. [CrossRef]
8. Wiesler, K.; Brandl, K.; Fleischmann, A.; Korber, N. Tetrahedral $[Tt_4]^{4-}$ Zintl Anions Through Solution Chemistry: Syntheses and Crystal Structures of the Ammoniates $Rb_4Sn_4 \cdot 2NH_3$, $Cs_4Sn_4 \cdot 2NH_3$, and $Rb_4Pb_4 \cdot 2NH_3$. *Zeitschrift für Anorganische und Allgemeine Chemie* **2009**, *635*, 508–512. [CrossRef]
9. Benda, C.B.; Henneberger, T.; Klein, W.; Fässler, T.F. $[Si_4]^{4-}$ and $[Si_9]^{4-}$ Clusters Crystallized from Liquid Ammonia Solution–Synthesis and Characterization of $K_8[Si_4][Si_9] \cdot (NH_3)_{14.6}$. *Zeitschrift für Anorganische und Allgemeine Chemie* **2017**, *643*, 146–148. [CrossRef]
10. Edwards, P.A.; Corbett, J.D. Stable homopolyatomic anions. Synthesis and crystal structures of salts containing the pentaplumbide (2-) and pentastannide (2-) anions. *Inorg. Chem.* **1977**, *16*, 903–907. [CrossRef]
11. Goicoechea, J.M.; Sevov, S.C. Naked Deltahedral Silicon Clusters in Solution: Synthesis and Characterization of Si_9^{3-} and Si_5^{2-}. *J. Am. Chem. Soc.* **2004**, *126*, 6860–6861. [CrossRef] [PubMed]
12. Suchentrunk, C.; Korber, N. Ge_5^{2-} Zintl anions: Synthesis and crystal structures of $[K([2.2.2]\text{-crypt})]_2Ge_5 \cdot 4NH_3$ and $[Rb([2.2.2]\text{-crypt})]_2Ge_5 \cdot 4NH_3$. *New J. Chem.* **2006**, *30*, 1737–1739. [CrossRef]
13. Joseph, S.; Suchentrunk, C.; Korber, N. Dissolving Silicides: Syntheses and Crystal Structures of New Ammoniates Containing Si_5^{2-} and Si_9^{4-} Polyanions and the Role of Ammonia of Crystallisation. *Z. Naturforsch.* **2010**, *B65*, 1059–1065. [CrossRef]
14. Henneberger, T.; Klein, W.; Fässler, T.F. Silicon Containing Nine Atom Clusters from Liquid Ammonia Solution: Crystal Structures of the First Protonated Clusters $[HSi_9]^{3-}$ and $[H_2\{Si/Ge\}_9]^{2-}$. *Z. Anorg. Allg. Chem.* **2018**, *644*, 1018–1027. [CrossRef]
15. Lorenz, C.; Hastreiter, F.; Hioe, J.; Nanjundappa, L.; Gärtner, S.; Korber, N.; Gschwind, R.M. Structure of $[HSi_9]^{3-}$ in the Solid State and its Unexpectedly High Dynamics in Solution. *Angew. Chem.* **2018**. [CrossRef] [PubMed]
16. Suchentrunk, C.; Daniels, J.; Somer, M.; Carrillo-Cabrera, W.; Korber, N. Synthesis and Crystal Structures Of The Polygermanide Ammoniates $K_4Ge_9 \cdot 9NH_3$, $Rb_4Ge_9 \cdot 5NH_3$ and $Cs_6Ge_{18} \cdot 4NH_3$. *Z. Naturforsch.* **2005**, *B60*, 277–283. [CrossRef]
17. Gärtner, S.; Suchentrunk, C.; Korber, N. Coordination preferences of the alkali cations sodium and caesium in the mixed-cationic Zintl ammoniate $Cs_{3.2}Na_{0.8}Ge_9 \cdot 5.3NH_3$. *Acta Crystallogr. C* **2014**, *70*, 1036–1039. [CrossRef] [PubMed]
18. Suchentrunk, C.; Korber, N. Synthesis and crystal structures of [K (18-crown−6)][Rb (18-crown−6)]$_2Ge_9 \cdot 6NH_3$, [Rb (18-crown−6)]$_3Ge_9 \cdot 9NH_3$ and [Cs (18-crown−6)]$_3Ge_9 \cdot 6NH_3$. *Inorg. Chim. Acta* **2006**, *359*, 267–272. [CrossRef]
19. Bentlohner, M.M.; Fischer, C.; Fässler, T.F. Synthesis and characterization of pristine closo-$[Ge_{10}]^{2-}$. *Chem. Commun.* **2016**, *52*, 9841–9843. [CrossRef] [PubMed]
20. Spiekermann, A.; Hoffinann, S.D.; Fässler, T.F. The Zintl ion $[Pb_{10}]^{2-}$: A rare example of a homoatomic closo cluster. *Angew. Chem. Int. Ed.* **2006**, *45*, 3459–3462. [CrossRef] [PubMed]
21. Ponou, S.; Fässler, T.F. Crystal Growth and Structure Refinement of K_4Ge_9. *Zeitschrift für Anorganische und Allgemeine Chemie* **2007**, *633*, 393–397. [CrossRef]
22. Queneau, V.; Sevov, S.C. Ge_9^{4-}: A deltahedral zintl ion now made in the solid-state. *Angew. Chem. Int. Ed.* **1997**, *36*, 1754–1756. [CrossRef]
23. Hoch, C.; Wendorff, M.; Röhr, C. Synthesis and crystal structure of the tetrelides $A_{12}M_{17}$ (A = Na, K, Rb, Cs; M = Si, Ge, Sn) and A_4Pb_9 (A = K, Rb). *J. Alloys Compd.* **2003**, *361*, 206–221. [CrossRef]

24. Von Schnering, H.G.; Baitinger, M.; Bolle, U.; CarrilloCabrera, W.; Curda, J.; Grin, Y.; Heinemann, F.; Llanos, J.; Peters, K.; Schmeding, A.; et al. Binary alkali metal compounds with the zintl anions Ge_9^{4-} and Sn_9^{4-}. *Z. Anorg. Allg. Chem.* **1997**, *623*, 1037–1039. [CrossRef]
25. Scharfe, S.; Fässler, T.F. Polyhedral nine-atom clusters of tetrel elements and intermetalloid derivatives. *Philos. Trans. R. Soc. A* **2010**, *368*, 1265–1284. [CrossRef] [PubMed]
26. Fässler, T.F. The renaissance of homoatomic nine-atom polyhedra of the heavier carbon-group elements Si-Pb. *Coord. Chem. Rev.* **2001**, *215*, 347–377. [CrossRef]
27. Esenturk, E.N.; Fettinger, J.; Eichhorn, B. Synthesis and characterization of the $[Ni_6Ge_{13}\cdot(CO)_5]^{4-}$ and $[Ge_9Ni_2(PPh_3)]^{2-}$ Zintl ion clusters. *Polyhedron* **2006**, *25*, 521–529. [CrossRef]
28. Geitner, F.S.; Klein, W.; Fässler, T.F. Synthesis and Reactivity of Multiple PR2-Functionalized Nonagermanide Clusters. *Angew. Chem. Int. Ed.* **2018**. [CrossRef]
29. Frischhut, S.; Klein, W.; Drees, M.; Fässler, T.F. Acylation of homoatomic Ge_9 Cages and Subsequent Decarbonylation. *Chem. Eur. J.* **2018**, *24*, 9009–9014. [CrossRef] [PubMed]
30. Sevov, S.C.; Goicoechea, J.M. Chemistry of deltahedral Zintl ions. *Organometallics* **2006**, *25*, 5678–5692. [CrossRef]
31. Goicoechea, J.M.; Sevov, S.C. Organozinc Derivatives of Deltahedral Zintl Ions: Synthesis and Characterization of closo-$[E_9Zn(C_6H_5)]^{3-}$ (E = Si, Ge, Sn, Pb). *Organometallics* **2006**, *25*, 4530–4536. [CrossRef]
32. Kocak, F.S.; Downing, D.O.; Zavalij, P.; Lam, Y.F.; Vedernikov, A.N.; Eichhorn, B. Surprising Acid/Base and Ion-Sequestration Chemistry of Sn_9^{4-}: HSn_9^{3-}, $Ni@HSn_9^{3-}$, and the Sn_9^{3-} Ion Revisited. *J. Am. Chem. Soc.* **2012**, *134*, 9733–9740. [CrossRef] [PubMed]
33. Xu, L.; Sevov, S.C. Oxidative coupling of deltahedral $[Ge_9]^{4-}$ Zintl ions. *J. Am. Chem. Soc.* **1999**, *121*, 9245–9246. [CrossRef]
34. Hauptmann, R.; Fässler, T.F. Low Dimensional Arrangements of the Zintl Ion $[Ge_9\text{-}Ge_9]^{6-}$ and Chemical Bonding in $[Ge_6]^{2-}$,$[Ge_9\text{-}Ge_9]^{6-}$, and $\{[Ge_9]\}^{2-}$. *Zeitschrift für Anorganische und Allgemeine Chemie* **2003**, *629*, 2266–2273. [CrossRef]
35. Ugrinov, A.; Sevov, S.C. $[Ge_9Ge_9Ge_9]^{6-}$: A Linear Trimer of 27 Germanium Atoms. *J. Am. Chem. Soc.* **2002**, *124*, 10990–10991. [CrossRef] [PubMed]
36. Yong, L.; Hoffmann, S.D.; Fässler, T.F. The Controlled Oxidative Coupling of Ge_9^{4-} Zintl Anions to a Linear Trimer $[Ge_9{=}Ge_9{=}Ge_9]^{6-}$. *Zeitschrift für Anorganische und Allgemeine Chemie* **2005**, *631*, 1149–1153. [CrossRef]
37. Ugrinov, A.; Sevov, S.C. $[Ge_9Ge_9Ge_9Ge_9]^{8-}$: A Linear Tetramer of Nine-Atom Germanium Clusters, a Nanorod. *Inorg. Chem.* **2003**, *42*, 5789–5791. [CrossRef] [PubMed]
38. Yong, L.; Hoffmann, S.D.; Fässler, T.F. Oxidative Coupling of Ge_9^{4-} Zintl Anions-Hexagonal Rod Packing of Linear $[Ge_9{=}Ge_9{=}Ge_9{=}Ge_9]^{8-}$. *Zeitschrift für Anorganische und Allgemeine Chemie* **2004**, *630*, 1977–1981. [CrossRef]
39. Downie, C.; Tang, Z.J.; Guloy, A.M. An Unprecedented $^1{}_\infty[Ge_9]^{2-}$ Polymer: A Link between Molecular Zintl Clusters and Solid-State Phases. *Angew. Chem. Int. Ed.* **2000**, *39*, 338–340. [CrossRef]
40. Downie, C.; Mao, J.G.; Parmar, H.; Guloy, A.M. The role of sequestering agents in the formation and structure of germanium anion cluster polymers. *Inorg. Chem.* **2004**, *43*, 1992–1997. [CrossRef] [PubMed]
41. Ugrinov, A.; Sevov, S.C. Synthesis of a chain of nine-atom germanium clusters accompanied with dimerization of the sequestering agent. *C. R. Chim.* **2005**, *8*, 1878–1882. [CrossRef]
42. Fässler, T.F.; Schiegerl, L.; Karttunen, A.; Tillmann, J.; Geier, S.; Raudaschl-Sieber, G.; Waibel, M. Charged Si_9 Clusters in Neat Solids and the Detection of $[H_2Si_9]^{2-}$ in Solution—A Combined NMR, Raman, Mass Spectrometric, and Quantum Chemical Investigation. *Angew. Chem. Int. Ed.* **2018**, *130*.
43. Spek, A.L. *Platon, A Multipurpose Crystallographic Tool*; Utrecht University: Utrecht, The Netherlands, 1998.
44. Agilent Technologies. *Crysalis Pro, Version 1.171.38.46*; Agilent Technologies: Santa Clara, CA, USA, 2017.
45. Hauptmann, R.; Fässler, T.F. Crystal structure of di [potassium([2.2.2]crypt)] tetrapotassium octadecagermanide (6-)–ethylenediamine solvate (1:6),$[K(C_{18}H_{36}N_2O_6)]_2K_4(Ge_9)_2\cdot 6C_2N_2H_8$. *Z. Kristallogr. NCS* **2003**, *218*, 461–463.
46. Nienhaus, A.; Hoffmann, S.D.; Fässler, T.F. First Synthesis of Group-14 Polyanions by Extraction of a Binary Alloy with dmf and a Novel Conformation of the $(Ge_9{-}Ge_9)^{6-}$ Dimer: Crystal Structures of $[K_6(Ge_9{-}Ge_9)](dmf)_{12}$,$[Rb_6(Ge_9{-}Ge_9)](dmf)_{12}$ and $[K_{2.5}Cs_{3.5}(Ge_9{-}Ge_9)](dmf)_{12}$. *Zeitschrift für Anorganische und Allgemeine Chemie* **2006**, *632*, 1752–1758. [CrossRef]

47. Scharfe, S.; Fässler, T.F. Synthesis of $(Ge_9–Ge_9)^{6-}$ Dimeric Zintl Ions in Liquid Ammonia Solutions of K_4Ge_9: Low-Dimensional Coordination Networks in the Crystal Structure of the Ammoniates $K_n[K([2.2.2]crypt)]_{6-n}[Ge_9–Ge_9](NH_3)_m$ (n = 2, 3, and 4). *Zeitschrift für Anorganische und Allgemeine Chemie* **2011**, *637*, 901–906. [CrossRef]
48. Benda, C.B.; Wang, J.Q.; Wahl, B.; Fässler, T.F. Syntheses and ^{1}H NMR Spectra of Substituted Zintl Ions $[Ge_9R_n]^{(4-n)-}$: Crystal Structures of $[Ge_9R]^{3-}$ (R = 2, 4, 6-$Me_3C_6H_2$, $CHCH_2$) and Indication of Tris-Vinylated Clusters. *Eur. J. Inorg. Chem.* **2011**, 4262–4269. [CrossRef]
49. Ugrinov, A.; Sevov, S.C. Rationally Functionalized Deltahedral Zintl Ions: Synthesis and Characterization of $[Ge_9–ER_3]^{3-}$,$[R_3E–Ge_9–ER_3]^{2-}$, and $[R_3E–Ge_9–Ge_9–ER_3]^{4-}$ (E = Ge, Sn; R = Me, Ph). *Chem. Eur. J.* **2004**, *10*, 3727–3733. [CrossRef] [PubMed]
50. Downie, C.; Mao, J.G.; Guloy, A.M. Synthesis and Structure of $[K^+$-(2,2) diaza-[18]-crown−6$][K_3Ge_9]$·2Ethylenediamine: Stabilization of the Two-Dimensional Layer $^2{}_\infty[K_3Ge_9{}^{1-}]$. *Inorg. Chem.* **2001**, *40*, 4721–4725. [CrossRef] [PubMed]
51. Ugrinov, A.; Sevov, S.C. $[Ph_2Bi–(Ge_9)–BiPh_2]^{2-}$: A Deltahedral Zintl Ion Functionalized by Exo-Bonded Ligands. *J. Am. Chem. Soc.* **2002**, *124*, 2442–2443. [CrossRef] [PubMed]
52. Wade, K. Structural and bonding patterns in cluster chemistry. *Adv. Inorg. Radiochem.* **1976**, *18*, 1–66.
53. Mingos, D.M.P. Polyhedral skeletal electron pair approach. *Acc. Chem. Res.* **1984**, *17*, 311–319. [CrossRef]
54. Hull, M.W.; Sevov, S.C. Functionalization of nine-atom deltahedral zintl ions with organic substituents: Detailed studies of the reactions. *J. Am. Chem. Soc.* **2009**, *131*, 9026–9037. [CrossRef] [PubMed]
55. Hull, M.W.; Sevov, S.C. Organo-zintl clusters soluble in conventional organic solvents: Setting the stage for organo-zintl cluster chemistry. *Inorg. Chem.* **2007**, *46*, 10953–10955. [CrossRef] [PubMed]
56. Hull, M.W.; Sevov, S.C. Addition of Alkenes to Deltahedral Zintl Clusters by Reaction with Alkynes: Synthesis and Structure of $[Fc–CH–CH–Ge_9–CH–CH–Fc]^{2-}$, an Organo-Zintl–Organometallic Anion. *Angew. Chem. Int. Ed.* **2007**, *46*, 6695–6698. [CrossRef] [PubMed]
57. Samanamu, C.R.; Amadoruge, M.L.; Yoder, C.H.; Golen, J.A.; Moore, C.E.; Rheingold, A.L.; Materer, N.F.; Weinert, C.S. Syntheses, structures, and electronic properties of the branched oligogermanes $(Ph_3Ge)_3GeH$ and $(Ph_3Ge)_3GeX$ (X = Cl, Br, I). *Organometallics* **2011**, *30*, 1046–1058. [CrossRef]
58. Hackspill, L. Sur quelques properiétés des métaux alcalins. *Helv. Chim. Acta* **1928**, *11*, 1003–1026. [CrossRef]
59. Suchentrunk, C.; Rossmier, T.; Korber, N. Crystal structures of the [18]-crown-6 ammoniate $C_{12}H_{24}O_6$·$2NH_3$ and the cryptand [2.2.2] ammoniate $C_{18}H_{36}O_6N_2$·$2NH_3$. *Z. Kristallogr.* **2006**, *221*, 162–165.
60. Kottke, T.; Stalke, D. Crystal handling at low temperatures. *J. Appl. Crystallogr.* **1993**, *26*, 615–619. [CrossRef]
61. Stalke, D. Cryo crystal structure determination and application to intermediates. *Chem. Soc. Rev.* **1998**, *27*, 171–178. [CrossRef]